HUMAN GENE THERAPY 20:225–237 (March 2009)

DOI: 10.1089/hum.2008.151

Transduction of Nonhuman Primate Brain with Adeno-Associated Virus Serotype 1: Vector Trafficking and Immune Response

Piotr Hadaczek,[1] John Forsayeth,[1] Hanna Mirek,[1] Keith Munson,[2,3] John Bringas,[1] Phil Pivirotto,[1] Jodi L McBride,[4] Beverly L. Davidson,[4] and Krystof S. Bankiewicz[1]

Abstract

We used convection-enhanced delivery (CED) to characterize gene delivery mediated by adeno-associated virus type 1 (AAV1) by tracking expression of hrGFP (humanized green fluorescent protein from *Renilla reniformis*) into the striatum, basal forebrain, and corona radiata of monkey brain. Four cynomolgus monkeys received single infusions into corona radiata, putamen, and caudate. The other group ($n = 4$) received infusions into basal forebrain. Thirty days after infusion animals were killed and their brains were processed for immunohistochemical evaluation. Volumetric analysis of GFP-positive brain areas was performed. AAV1-hrGFP infusions resulted in approximately 550, 700, and 73 mm^3 coverage after infusion into corona radiata, striatum, and basal forebrain, respectively. Aside from targeted regions, other brain structures also showed GFP signal (internal and external globus pallidus, subthalamic nucleus), supporting the idea that AAV1 is actively trafficked to regions distal from the infusion site. In addition to neuronal transduction, a significant nonneuronal cell population was transduced by AAV1 vector; for example, oligodendrocytes in corona radiata and astrocytes in the striatum. We observed a strong humoral and cell-mediated response against AAV1-hrGFP in transduced monkeys irrespective of the anatomic location of the infusion, as evidenced by induction of circulating anti-AAV1 and anti-hrGFP antibodies, as well as infiltration of $CD4^+$ lymphocytes and upregulation of MHC-II in regions infused with vector. We conclude that transduction of antigen-presenting cells within the CNS is a likely cause of this response and that caution is warranted when foreign transgenes are used as reporters in gene therapy studies with vectors with broader tropism than AAV2.

Introduction

The delivery of genes into the CNS offers an attractive potential option for the treatment of various neurological disorders. Efficient distribution of therapeutic vectors within the brain is critical, especially in diseases that may require neuronal targeting of large anatomical regions of the brain (e.g., neurodegenerative diseases, lysosomal storage disorders, and stroke). Viral vectors that are able to convey robust gene transfer must be combined with efficient brain delivery systems for effective translation of gene therapy technology into the clinic.

Adeno-associated virus (AAV) was developed as a gene transfer vehicle through the pioneering work of Samulski and colleagues after they isolated and characterized a clone of AAV serotype 2 (AAV2) (Samulski *et al.*, 1982, 1983). In 1994, recombinant AAV was first used to transduce neurons (Kaplitt *et al.*, 1994) and it has proven a useful vector for gene transfer to the brain. Many studies have evaluated a number of different AAV serotypes in a variety of animal models of neurological disease (Davidson and Breakefield, 2003). At present, eight serotypes of AAV have been evaluated as recombinant vectors (AAV1–AAV8) and many more have been isolated from various species including nonhuman primates (Grimm and Kay, 2003; Mori *et al.*, 2004). True AAV serotypes include AAV1–5 and AAV7–9, although variants AAV6, AAV10, and AAV11 do not fit the serotype definition, sharing serology with others, or being poorly characterized (Wu *et al.*, 2006a). Reviews (Grimm and Kay, 2003; Gao *et al.*, 2005) have improved our understanding of AAV serotypes with respect

[1]Laboratory of Molecular Therapeutics, Department of Neurosurgery, University of California, San Francisco, San Francisco, CA 94103.
[2]Targeted Genetics, Seattle, WA 98101.
[3]Present address: Allozyne, Seattle, WA 98102.
[4]Department of Internal Medicine, University of Iowa, Iowa City, IA 52242.

to their isolation, serology, classification, and potential application to gene therapy. Comparative analysis of AAV transduction in the brain has demonstrated differences in cellular tropism (Davidson *et al.*, 2000). On the basis of their desirable properties, correct selection of a specific serotype should fit specific treatment requirements (type of brain cells affected by a disease, level of transduction, anatomical sites, etc.).

In designing optimal conditions for delivering viral vectors to the CNS, the method of vector delivery is as important as the vector itself. Convection-enhanced delivery (CED) has proven to be an efficient way to deliver therapeutic agents (including viral vectors) into the brain (Lieberman *et al.*, 1995; Bankiewicz *et al.*, 2000; Cunningham *et al.*, 2000; Nguyen *et al.*, 2001; Hadaczek *et al.*, 2006a). CED uses a pressure gradient established at the tip of an infusion catheter that initially creates bulk flow that "pushes" the viral particles through the space between brain cells (i.e., the extracellular space) (Bobo *et al.*, 1994). The pressurized infusate then engages the perivascular space and distribution is significantly aided by the pulsation of blood vessels. We have shown previously that pulse pressure appears to be the main driver of CED (Hadaczek *et al.*, 2004). As a result, the vector is distributed evenly, and at higher concentrations over a larger area, than in the absence of CED, that is, by diffusion alone. This active process results in effective trafficking of vector from sites of injection to locations some distance away.

The present study formed part of a broader program to develop a gene-silencing approach for the treatment of Huntington's disease (HD). In order for such an approach to be clinically effective, it seemed likely that widespread expression in target regions of the brain, cortex, and striatum would be needed. It has been reported that the transduction efficiency in the CNS of AAV1 is superior to that of AAV2 in various animal models, including mouse, rat, and cat (Vite *et al.*, 2003; Wang *et al.*, 2003; Burger *et al.*, 2004). Significantly, however, there is to our knowledge no published report of AAV1 in the primate brain.

We therefore designed our experiments to investigate how AAV1 delivered by CED performed in the monkey brain in regions relevant to Huntington's disease (HD). Accordingly, AAV1-hrGFP was convected into corona radiata, striatum, and basal forebrain. (*Note:* The verb *to convect* is used here to describe the distribution of an infused substance or particle in a target tissue by means of CED.) Infusion into the corona radiata is known to disseminate nanoliposomes within the white matter to reach deep cortical regions from within the underlining neuronal fiber tracts (Krauze *et al.*, 2005; Saito *et al.*, 2005). Moreover, retrograde axonal transport of AAV and/or gene product has been reported by Kaspar and colleagues (2002) and others (Burger *et al.*, 2004; Passini *et al.*, 2005). We also targeted basal forebrain with the expectation that AAV1 would be anterogradely transported into the cortical regions. Conversely, retrograde axonal transport to the cortex was tested in animals in which striatal transduction was achieved. In the course of our experiments, we detected a strong cell-mediated response against AAV1-hrGFP in target brain regions, as well as a humoral response against both hrGFP and AAV1 capsid. This response probably arose from transduction of nonneuronal antigen-presenting cells by the vector. We conclude that, although this does not preclude consideration of broad AAV serotypes with broad tropism in the CNS, caution is warranted in the design of *in vivo* experiments, particularly when foreign reporter genes are used.

Materials and Methods

Experimental subjects and study design

This protocol was reviewed and approved by the Institutional Animal Care and Use Committee (University of California, San Francisco, San Francisco, CA). Eight cynomolgus monkeys (3–8 kg) were used. The experimental design included convection-enhanced delivery (CED) of AAV1-hrGFP (adeno-associated virus type 1 carrying the humanized *Renilla reniformis* green fluorescent protein) into the monkey brain (detailed study design is described subsequently).

Study design

To examine the distribution of hrGFP transduction within the monkey brain under study conditions, we assigned animals to two separate study groups (Table 1).

Plasmid and AAV1-hrGFP production

pAAV-CMV-hrGFP carries the humanized GFP from *Renilla reniformis* under the control of the human cytomegalovirus (CMV) major immediate-early gene enhancer/promoter region, a chimeric human β-globin eGFP expression cassette followed by the splice donor/human immunoglobulin splice acceptor site, and a bovine growth hormone poly(A) signal. Recombinant AAV1 vector was produced by a standard calcium phosphate transfection method in adherent human 293 cells, with adenovirus helper, *trans*-packaging, and AAV vector plasmid. Briefly, cells were seeded in 225-cm^2 T-flasks and grown to subconfluency in complete Dulbecco's modified Eagle's medium (DMEM; Cambrex Bio Science Walkersville, Walkersville, MD). Plasmids pAd helper 4.1 and pBS-HSP-RC2.3, and vector plasmid (i.e., pAAV-CMV-hrGFP), were added (2:2:1 molar ratio) to a 300 m*M* $CaCl_2$ solution. To form a calcium phosphate precipitate, the plasmid mixture was added to a 2× HBS buffer (280 m*M* NaCl, 1.5 m*M* Na_2PO_4, 5 m*M* HEPES; pH 7.1), incubated for 30 sec, and then added directly onto the 293 cell monolayer. The cells were incubated for 6 to 8 hr at 37°C, after which medium was aspirated and replenished with fresh serum-free DMEM. Three days after transfection, the cells were lysed by the addition of deoxycholate (Fisher Scientific, Houston, TX) to a final concentration of 0.5% (w/v), releasing all cellular and nuclear contents into the solution. The cellular DNA was digested by the addition of Benzonase (EMD Biosciences, Gibbstown, NJ) at a concentration of 10 U/ml for 1 hr at 37°C. Tween 20 (Fisher Scientific, Santa Clara, CA) was added to a final concentration of 1% (v/v) with a further incubation for 60 min at 37°C, followed by the addition of NaCl to a final concentration of 1 *M*, before clarification through depth filters (Millipore, Bedford, MA). Clarified lysates were concentrated 15- to 20-fold by tangential flow filtration with Pellicon 2 minicassettes (110-kDa cutoff; Fisher Scientific, Houston, TX) and were exchanged against formulation buffer (20 m*M* Tris [pH 8.0], 0.2 *M* NaCl, 2 m*M* $MgCl_2$, and 2% [v/v] glycerol). The lysates were filtered through a 0.45-μm SuporCap filter unit (Gelman; Pall Life Sciences, Ann Arbor, MI) and stored at −80°C. The harvested lysates were purified by ion-exchange chromatog-

Table 1. Study Groups and Conditions for Intracerebral Infusions of AAV1-hrGFP in Monkeys by Convection-Enhanced Delivery

Study group	Infused brain regions (right hemisphere)[a]	CED parameters		
		Rate (time)	Total volume and dose of AAV1 per site	Total infusion time per site (min)
A ($n=4$)	Corona radiata (1 site)	0.2 μl/min (10 min) 0.5 μl/min (10 min) 0.8 μl/min (10 min) 1.0 μl/min (10 min) 1.5 μl/min (10 min) 2.0 μl/min (10 min) 2.5 μl/min (10 min) 3.0 μl/min (22 min)	150 μl (6.9×10^{11} DRP)	92
	Caudate (1 site)	0.2 μl/min (10 min) 0.5 μl/min (10 min) 0.8 μl/min (10 min)	50 μl (2.3×10^{11} DRP)	55
	Putamen (2 sites)	1.0 μl/min (10 min) 1.5 μl/min (10 min) 2.0 μl/min (5 min)		
B ($n=4$)	Basal forebrain (2 sites)	1.0 μl/min (10 min)	10 μl (4.6×10^{10} DRP)	10

Abbreviations: CED, convection-enhanced delivery; DRP, DNase-resistant particles.
[a]Control left hemispheres were infused with PBS (same conditions as for right hemispheres).

raphy as previously described (Kaludov *et al.*, 2002; Zolotukhin *et al.*, 2002). Eluted vector was formulated in a buffer containing 20 m*M* Tris (pH 8.0), 0.2 *M* NaCl, 2 m*M* $MgCl_2$, and 2% (v/v) glycerol and aseptically filtered. Final vector preparation was >95% pure, with low endotoxin level (<0.5 unit/ml). The purified vector was not significantly aggregated, as determined by dynamic laser light-scattering analysis with a DynaPro-99 instrument (Protein Solutions, High Wycombe, UK). Vector titer was determined by real-time polymerase chain reaction (PCR) with a Prism 7900 sequence detector (Applied Biosystems, Foster City, CA) and the final concentration (lot 05-0530) was 4.6×10^{12} DNase-resistant particles (DRP)/ml.

Surgical procedures

Cannula design, preparation of loading lines, and cerebral infusion of AAV1-hrGFP were performed as previously described (Hadaczek *et al.*, 2006a). Multiple needle cannulas attached to holders were stereotactically guided to brain target sites. The infusion parameters are shown in Table 1.

Histological procedures

Animals were deeply anesthetized with sodium pentobarbital (25 mg/kg, intravenous) and killed 4 weeks after AAV1-hrGFP administration. The brains were removed and placed in the brain mold, and sectioned coronally into 6-mm slices. The slices were postfixed in Zamboni's fixative for 24 hr, washed briefly in PBS, and adjusted in an ascending sucrose gradient (10, 20, 30%) before storage at −80°C. Fixed brain slices were cut into 40-μm coronal sections with a cryostat. Sections were collected in series. Each section was stored in cryoprotectant sucrose solution at −80°C. Humanized rGFP (hrGFP) was detected by means of a fluorescence microscope without further staining (native fluorescence). To evaluate the cell types transduced, sections were processed for fluorescence immunostaining with various markers. Every tenth section was washed in phosphate-buffered saline (PBS) and incubated in Sniper blocking solution (Biocare Medical, Concord, CA) for 20 min, followed by overnight incubation in primary antibody solution: (1) anti-S-100, a marker for astrocytes (rabbit polyclonal, diluted 1:300; Biocare Medical); (2) anti-neuronal nuclei (NeuN), a marker for neurons (mouse monoclonal, diluted 1:250; Chemicon International/Millipore, Temecula, CA); (3) anti-human oligodendrocyte transcription factor-2 (Olig2), a marker for oligodendrocytes (goat polyclonal, diluted 1:20; R&D Systems, Madison, WI). The next day, sections were washed in PBS with 2% goat serum and 0.01% Triton-X (three times, 5 min each), and incubated in secondary antibody for 1 hr (tetramethylrhodamine isothiocyanate [TRITC]-conjugated goat anti-mouse, goat anti-rabbit, or donkey anti-goat IgG [diluted 1:100; Jackson Laboratory, Bar Harbor, ME]). After three washes in PBS with 0.01% Triton-X, sections were mounted on slides, coverslipped, and examined by fluorescence microscopy. For nuclear counterstaining, 4′,6-diamidino-2-phenylindole (DAPI) working solution (100 ng/ml in PBS) was used for the last wash. To assess neuroinflammation four markers were used: (1) CD68 (mouse monoclonal, diluted 1:1000; Dako, Carpinteria, CA), (2) Iba1 (rabbit polyclonal, diluted 1:1000; Biocare Medical), (3) CD4 (mouse monoclonal, diluted 1:50; Biocare Medical), and (4) MHC-II (mouse monoclonal, diluted 1:75; United States Biological, Marblehead, MA). Standard diaminobenzidine tetrahydrochloride (DAB) staining was used for visualization (kit and protocol from Vector Laboratories, Burlingame, CA). For the last two antibodies mentioned, heat antigen retrieval was performed (80°C for 20 min in Diva solution; Biocare Medical). A fluorescence enhancement system was used to increase the signal (protocol from Biocare Medical with a secondary antibody, DyLight 549 [Pierce Biotechnology/Thermo Fisher Scientific, Rockford, IL]). In addition, standard hematoxylin–eosin (H&E) staining was performed on every tenth section.

Fluorescence microscopy was used to determine the number of single- and double-labeled cells in sections. Ten random pictures were taken (objective, ×20) from each monkey for each marker evaluated (one picture for every tenth section mounted on a slide). The images were printed on Highland transparency films (3M, St. Paul, MN) from the three different fluorescence channels (DAPI, FITC, and rhodamine). Counts of double-labeled cells were made on merged images from various combinations of channels. At least 1000 cells were counted for each marker.

BrainLAB image analysis

Areas expressing hrGFP on primate histology sections were (manually) delineated on primate CNS magnetic resonance imaging (MRI) scans with BrainLAB software (BrainLAB, Heimstetten, Germany). Software allowed three-dimensional reconstruction of hrGFP expression on MRI and analysis of volume of transduction (V_t). This method (Hadaczek *et al.*, 2006a) has proven to be as precise as quantification of V_t calculated from consecutive histological sections by the method of Cavalieri (Cavalieri, 1996; Grimm and Kay, 2003).

Volumetric measurements of monkey basal ganglia

To calculate the volume of the monkey basal ganglia (putamen, caudate, internal and external globus pallidus), volumetric measurements were made on the basis of MRI scans. Four monkey brains from group A were subjected to MR imaging (Signa 1.5T; GE Healthcare Life Sciences, Piscataway, NJ). As noted previously, BrainLAB software was used to delineate basal ganglia of the right hemisphere and to calculate its volume for each monkey. On this basis, the average volume of the monkey basal ganglia was found to be 1.36 cm^3. One monkey (Healy) was not taken into consideration as the signal from hrGFP was not detectable (this animal was not used for calculation of V_t).

Neutralizing antibody assay

Serum samples were collected before surgery (baseline) and on day 30 (euthanasia). The reporter virus AAV1-hrGFP (at a multiplicity of infection equal to 1×10^5 DRP/cell) was preincubated with heat-inactivated sera for 1 hr at 37°C. After incubation in serial serum dilutions, virus was added to 293 cells in 96-well plates for 48 hr. A fluorescence plate reader (FLx800; BioTek Instruments, Winooski, VT) was used to quantify the intensity of hrGFP signal expressed by the cultured cells. Neutralizing antibody titers were reported as the highest serum dilution that inhibited transduction by 50% of that seen with serum from a naive animal.

Dot-blot analysis

Antibodies directed against the transgene, hrGFP, were detected by immunodot blotting as follows. After transducing HEK-293 cells with AAV1-hrGFP (1×10^4 DRP/cell), cells were harvested 4 days later and a protein extract was prepared. Two microliters of the extract was applied as a dot to wet polyvinylidene difluoride (PVDF) membrane (Bio-Rad, Hercules, CA) cut into 9×9 mm squares, and allowed to dry. Subsequent immunoblotting was based on the instruction manual for the Opti-4CN substrate kit (Bio-Rad). Monkey sera, collected at euthanasia, were diluted accordingly: 1:100, 1:500, 1:1000, 1:2000, 1:4000, and 1:8000 and used as a primary antibody. Horseradish peroxidase (HRP)-conjugated goat anti-human IgG was used as a secondary antibody at 1:3000 dilution. After colorimetric development, dot-blots were photographed and the intensities of the signals produced were compared against serum titer. Sera from two naive monkeys were used as negative controls. To confirm the specificity against hrGFP, a polyclonal antibody raised against hrGFP (Stratagene, La Jolla, CA) was used as a positive control. No other available GFP-related antibodies reacted with hrGFP (data not shown).

Results

CED was used to infuse AAV1-hrGFP into the striatum (putamen and caudate) and corona radiata (group A) as well as into basal forebrain (group B) of eight monkeys (four monkeys per group). Four weeks after surgery, the distribution of hrGFP expression within the brain was analyzed by fluorescence. The analysis of volume of transduction (V_t) was determined as described (see Materials and Methods).

Distribution of hrGFP within the brain

In group A, hrGFP-positive cells were observed in all three targeted structures: caudate, putamen, and corona radiata. Infusion of 150 μl of the vector resulted in transduction of 548 ± 89 mm^3 ($n=4$) of the corona radiata (CR). Consequently, the V_i:V_t ratio (volume of infusion to volume of transduction) was 1:3.6 (150-mm^3 infusion resulted in ~550-mm^3 transduction). Similar ratios (Table 2) were observed in striatum (1:4.7, where $V_i=150$ mm^3 and $V_t=707\pm125$ mm^3)

Table 2. Volume of Transduction within Infused Brain Structures

Monkey (group A)	*Corona radiata (n = 4)*	*Striatum*[a] *(n = 3)*	*Monkey (group B)*	*Basal forebrain (n = 4)*
Marten	809 mm^3	768 mm^3	Benz	68 mm^3
Healy	424 mm^3	N/A	Bugatti	60 mm^3
Aston	449 mm^3	887 mm^3	Ghia	83 mm^3
Daimler	509 mm^3	466 mm^3	Jensen	80 mm^3
Mean ± SE	548 ± 89 mm^3	707 ± 125 mm^3	**Mean ± SE**	73 ± 5 mm^3
V_i:V_t	1:3.6	1:4.7	V_i:V_t	1:3.6

Abbreviations: N/A, due to technical problems with the infusion lines, the striatal region was not transduced and therefore we were unable to calculate the V_t; V_i, volume of infusion; V_t, volume of transduction.

[a]Transduced area includes also neighboring brain structures (internal and external globus pallidus, subthalamic nucleus, internal capsule) where signal was observed due to the transport from the infusion sites.

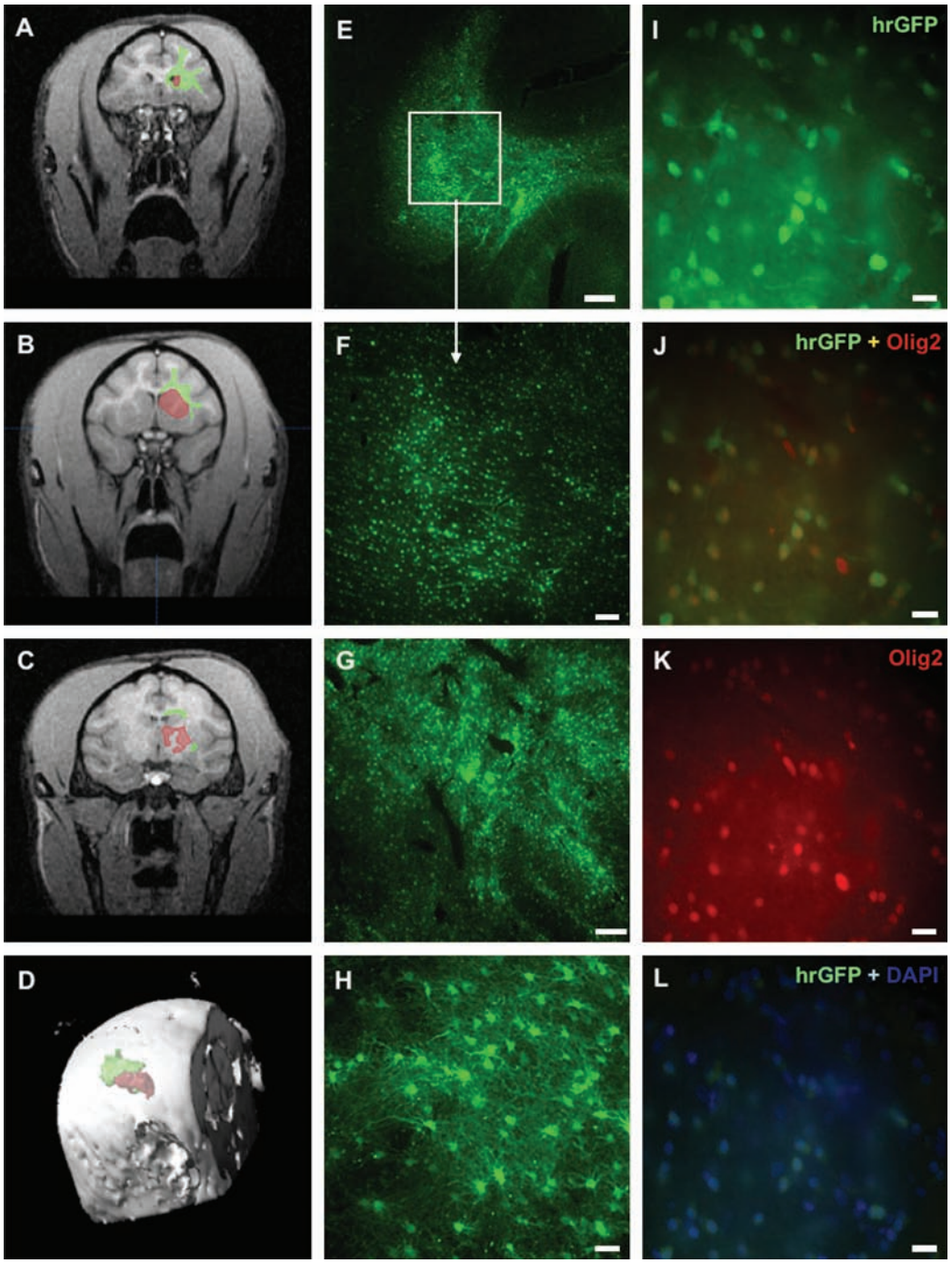

FIG. 1. Distribution of hrGFP (humanized green fluorescent protein from *Renilla reniformis*) transduction after convection-enhanced delivery (CED) of AAV1-hrGFP into the monkey brain. (**A–C**) Areas of transduction of hrGFP within corona radiata (green) and striatum (red) were outlined on brain MRI scans by means of BrainLAB software (from histological sections). Three scans from different brain levels (coronary plane) are shown from a representative monkey (group A). (**D**) The software allowed three-dimensional reconstruction of hrGFP expression on MRI and calculation of the volume of transduction (V_t) within the targeted brain structures. (**E**) Brain section (40 μm) of a representative monkey showing robust transduction of hrGFP within corona radiata (CR). Scale bar: 1 mm. (**F**) Higher magnification of the same section. Scale bar: 200 μm. (**G**) Robust transduction of AAV1-hrGFP within the striatum in a representative monkey (group A). Scale bar: 500 μm. (**H**) Higher magnification from striatum (group A), showing nonneuronal transduction (lack of costaining with NeuN; data not shown). Costaining with S-100 verified astrocytic lineage (see Fig. 2A–C for confirmation). Scale bar: 50 μm. (**I–L**) Colabeling of the transduced cells within CR (group A). On the basis of DAPI staining, the efficiency of transduction was 55.6% [(**L**) cells positive for both hrGFP and DAPI]. Approximately 88% of the target cells were oligodendrocytes [(**J**) cells positive for both hrGFP and Olig2]. Scale bars: 25 μm.

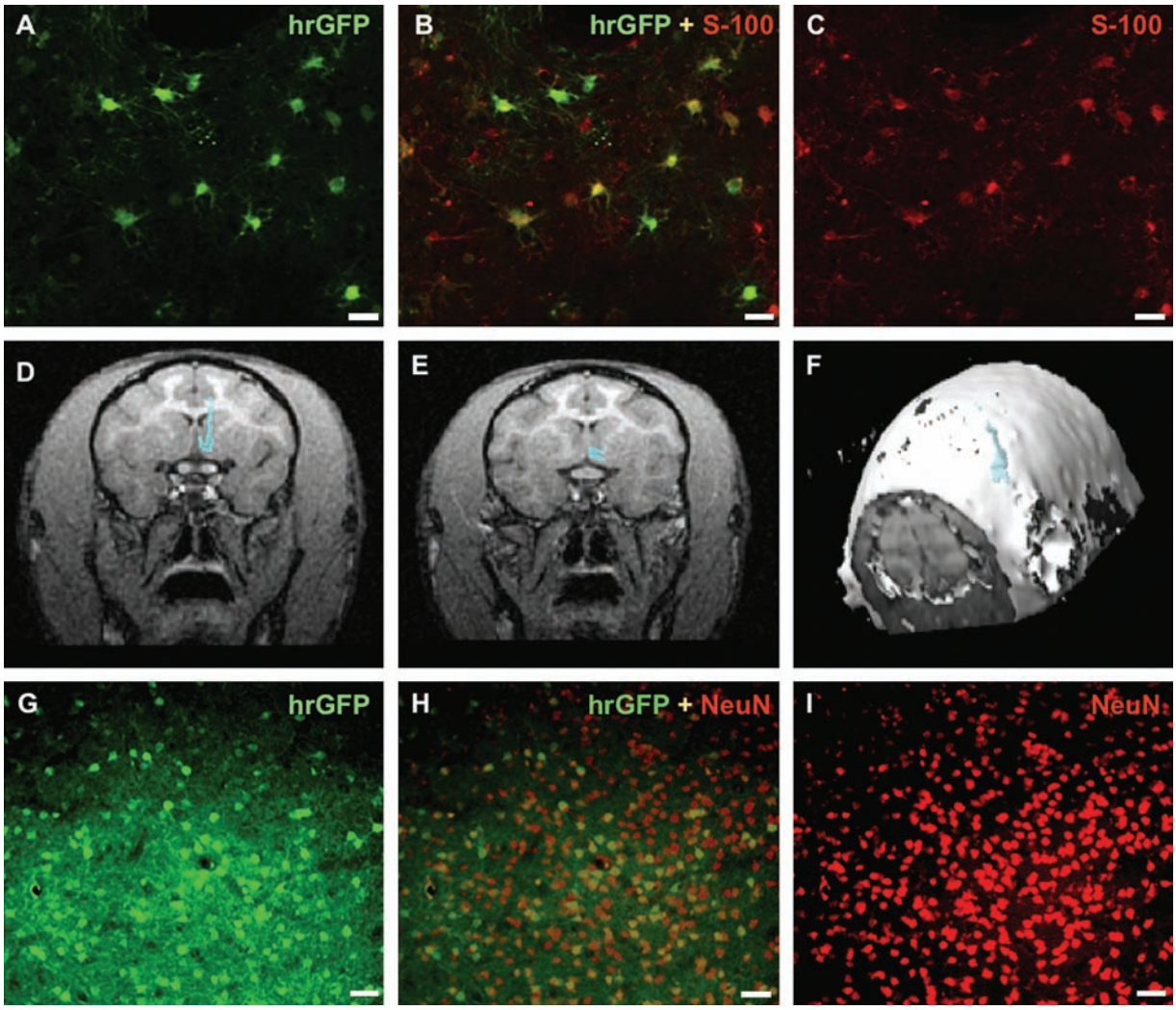

FIG. 2. Distribution of hrGFP transduction in the striatum and basal forebrain. (**A–C**) Costaining with antibody against S-100 (astrocytic marker) confirmed nonneuronal transduction of AAV1-hrGFP within the striatum (monkey Aston). Scale bars: 25 μm. (**D** and **E**) Areas of transduction (blue) of hrGFP (group B) were delineated on CNS MRI scans with BrainLAB software. Two consecutive MRI scans are shown. (**F**) The software allowed three-dimensional reconstruction of hrGFP expression on MRI and calculation of the volume of transduction (V_t) as 80 mm^3. (**G–I**) Immunohistochemical costaining with nuclear marker, NeuN, confirmed neuronal transduction (group B). Approximately 37.5% neurons within basal forebrain were transduced. Scale bars: 50 μm.

and basal forebrain (group B) (1:3.6, where $V_i = 20$ mm^3 and $V_t = 73 \pm 5$ mm^3); see also Figs. 1A–D and 2D–F. To calculate the proportion of striatum (basal ganglia) transduced with the AAV1-hrGFP vector, we measured the volume of monkey striatum (including internal and external globus pallidus and internal capsule) from MRI scans. The mean volume of all these structures forming the basal ganglia from one hemisphere was 1360 mm^3. The transduced area accounted for more than 50% of the entire basal ganglia (707 mm^3).

Efficiency of transduction and cell type specificity

To evaluate the efficiency of transduction, we calculated the number of cells transduced within a particular brain structure. We used various antibodies as cell markers to identify the specificity of AAV1 for various brain cells. The transduction efficiency of AAV1-hrGFP was 55.6% within the corona radiata (based on DAPI and hrGFP costaining; Fig. 1L). Further assessment demonstrated that 88.2% of the target cells were oligodendrocytes, indicated by costaining with Olig2 marker (Fig. 1I–K). Only a small percentage of cells expressing hrGFP costained with S-100 (marker for astrocytes). Interestingly, GFP fluorescence can be significantly reduced by formalin fixation. Thus, staining with anti-GFP antibodies is necessary to visualize GFP expression when formalin-based fixatives are used. In the present case, however, we used humanized *R. reniformis* GFP, a more stable variant of GFP used as a common reporter gene. In comparison with our previous studies with eGFP, we found that hrGFP gave a signal sufficient for visualization without the need for immunohistochemistry. When the striatum (caudate and putamen) was targeted, astrocyte transduction predominated to an overwhelming extent (Fig. 1G and H as well as Fig. 2A–C) with only sporadic neuronal transduction (Fig. 3A–C), in striking contrast to our

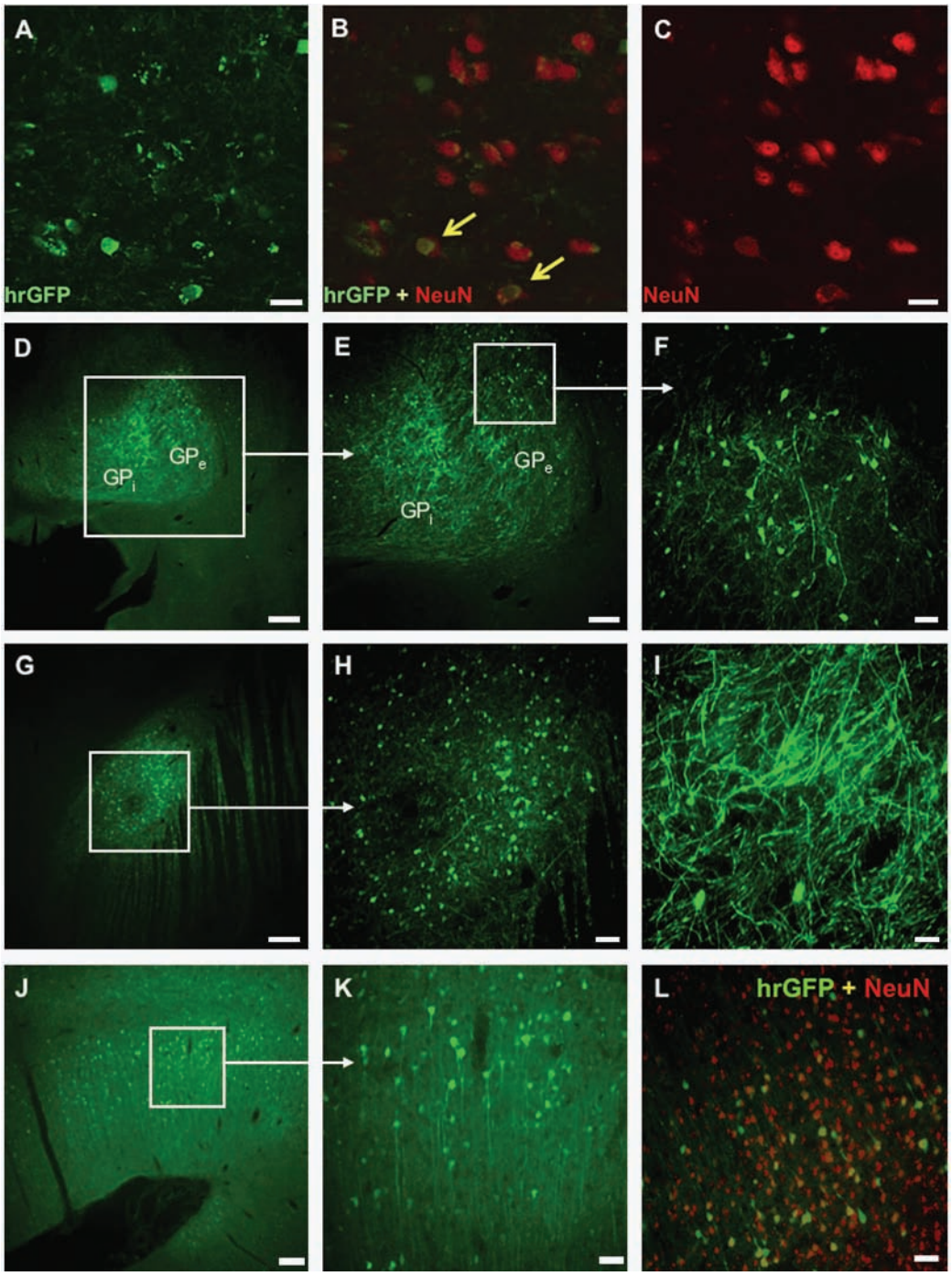

FIG. 3. Transduction of striatal neurons with AAV1-hrGFP. (**A**–**C**) Only a small percentage of the transduced cells within monkey striatum were neurons. Arrows indicate neurons ($NeuN^+$) expressing hrGFP. Scale bars: 50 μm. (**D** and **E**) Signal for hrGFP was detected both in internal (GP_i) and external (GP_e) globus pallidus. (**F**) Higher magnification of the transduced region of GP_e. Neuronal transduction was confirmed with NeuN staining (data not shown). Scale bars: (**D**) 1 mm; (**E**) 500 μm; (**F**) 100 μm. (**G**–**I**) Transport of AAV1-hrGFP to the subthalamic nucleus. Nuclear costaining with NeuN confirmed neuronal transduction (data not shown). Aside from a strong hrGFP signal within cell bodies, numerous neuronal fibers were also clearly fluorescent (**I**). Scale bars: (**G**) 500 μm; (**H**) 100 μm; (**I**) 50 μm. (**J**) Transduction of cortical regions of the monkey brain. After infusion of AAV1-hrGFP into the corona radiata, the hrGFP signal was also detected within the neurons of deeper cortical regions neighboring the corona radiata. Infusions of viral vectors into the white matter tracts can be a solution for targeting large cortical areas of the brain. Scale bar: 200 μm. (**K**) Higher magnification of the cortical region selected in (**J**), showing transduced neurons. Scale bar: 50 μm. (**L**) Within this transduced cortical area, nearly 40% of all $NeuN^+$ cells were also $hrGFP^+$. Scale bar: 50 μm.

Table 3. Trafficking of AAV1-hrGFP within Monkey Brain after Intracerebral Convection-Enhanced Delivery

Group	Target	Trafficking to:	Marker		
			NeuN	S-100	Olig2
A	Corona radiata Oligodendrocytes Astrocytes	Deep cortical regions neighboring with corona radiata	+	–	–
	Striatum Astrocytes (predominant) Neurons (sporadic)	GPe, GPi, STN, MFB, IC, AC	+	–	–
B	Basal forebrain Neurons Astrocytes	No trafficking to other brain structures was observed	–	–	–

Abbreviations: GPe, globus pallidus external; GPi, globus pallidus internal; STN, subthalamic nucleus; MFB, medial forebrain bundle; IC, internal capsule; AC, anterior commissure; NeuN, neuronal nuclei; S-100, marker for astrocytes; Olig2, oligodendrocyte transcription factor-2.

experience with AAV2 (Bankiewicz *et al.*, 2000, 2003; Hadaczek *et al.*, 2006a). In monkeys from group B, infusion of 20 μl of AAV1-hrGFP into the basal forebrain resulted in transduction of 37.5% of the neurons (both hrGFP$^+$ and NeuN$^+$) within this region of the brain (Fig. 2G–I). We also observed a small percentage of transduced astrocytes. Table 3 summarizes cell tropism for AAV1-hrGFP in the three infused brain regions.

Vector trafficking

Infusion of vector into the putamen resulted in widespread expression of reporter hrGFP in both the external and internal globus pallidus (Table 3 and Fig. 3D–F), the subthalamic nucleus, the medial forebrain bundle, and both the internal capsule and anterior commissure (Fig. 3G–I). In the corona radiata, which contains no neuronal cell bodies, only transduction of oligodendrocytes and astrocytes was observed (Fig. 1E, F, and I–L). However, neighboring deep layers of cortical neurons adjacent to the corona radiata displayed transduced neurons (Fig. 3J–L). Interestingly, in this neighboring region, only neurons were hrGFP$^+$, with 39.5% of all NeuN$^+$ cells doubly positive. In contrast, no transport to other brain structures was observed in monkeys from group B, in which vector was infused into basal forebrain, and where neuronal transduction was predominant but not exclusive. We attribute the lack of trafficking outside this region to the small volume (dose) of vector infused. The small volume of the basal forebrain necessitated infusion of only a small volume of infusate.

Immune response against AAV1-hrGFP

Infusion of AAV2 into rodent and nonhuman primate brain by CED triggers in most cases a significant humoral response against AAV2 capsid (Sanftner *et al.*, 2004; Cunningham *et al.*, 2008). We wanted to determine whether this was also true for AAV1. We used a neutralizing antibody (NAb) assay to determine the level of circulating antibodies directed against AAV1 capsid, measured before (baseline) and 1 month after transduction. All monkeys showed elevated level of NAb 1 month after surgery. In general, monkeys from group A (high vector dose) had higher titers of NAb in comparison with the animals transduced with low-dose vector (group B); see Table 4 for details.

Because hrGFP is a foreign antigen and AAV1, in contrast to AAV2, transduces nonneuronal cells that presumably include antigen-presenting cells (APCs), we asked whether animals infused with AAV1-hrGFP also had significant titers of antibodies against hrGFP. We used a dot-blot assay to detect antibodies against the transgene. Sera from monkeys whose brains were transduced with AAV1-hrGFP contained antibodies against hrGFP, whereas no reaction was observed with sera from naive animals (not transduced with AAV1-hrGFP). The titer of sera from group A was stronger than that of group B (Fig. 4A and B). In general, a dilution of 1:8000 of the A group

Table 4. Neutralizing Antibodies Directed against AAV1 Capsid before and after Transduction with AAV1-hrGFP

Monkey	Presurgery NAb AAV1 titer (baseline)	Postsurgery NAb AAV1 titer
	Group A (high vector dose)	
Aston	1:4	≥1:512
Healy	1:4	≥1:512
Daimler	1:8	≥1:512
Marten	1:4	1:128
	Group B (low vector dose)	
Benz	1:32	1:128
Bugatti	1:8	1:256
Ghia	1:32	≥1:512
Jensen	1:8	1:16

Abbreviation: NAb, neutralizing antibody.

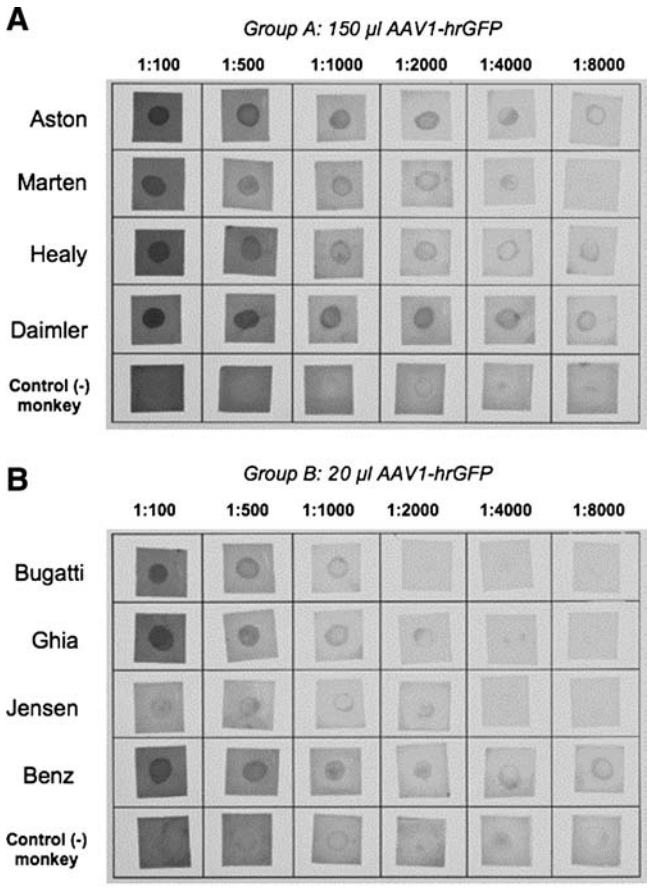

FIG. 4. Dot-blot assay of individual sera from monkeys transduced with AAV1-hrGFP. Monkeys from group A evinced a higher titer of the anti-hrGFP antibodies than those from group B, reflecting perhaps the greater amount of immunogenic hrGFP being produced by the transduced cells. Sera from two naive monkeys were used as negative control.

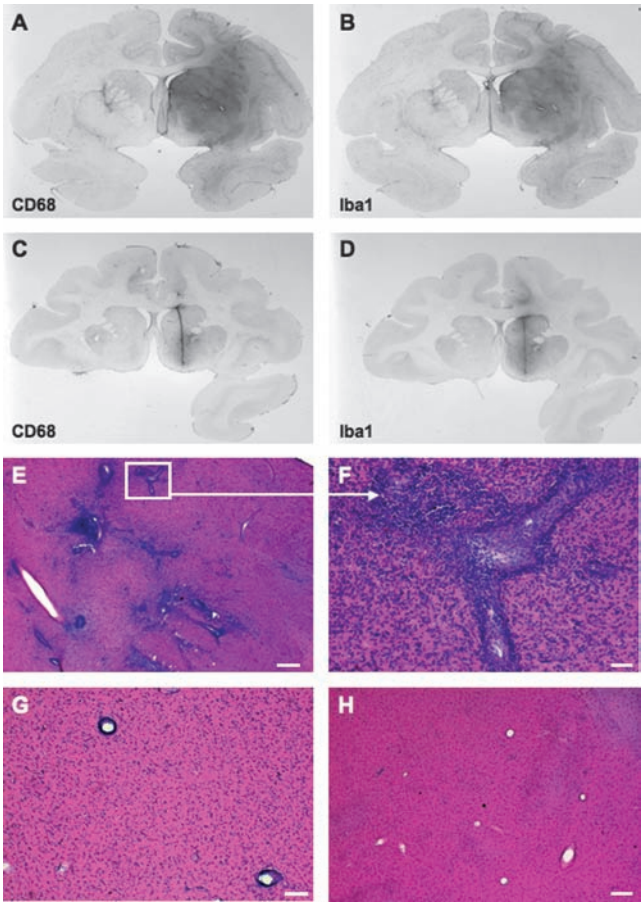

FIG. 5. Neuroinflammation within monkey brain after transduction with AAV1-hrGFP. (**A** and **B**) Sections (group A) were stained against CD68 (**A**), a marker for infiltrating macrophages, and against Iba1 (**B**), a marker for microglia. (**C** and **D**) Staining against CD68 and Iba1, respectively (group B). Signal is localized to the needle track (small volume of the vector was infused in this group (20 μl) whereas in group A, as much as 300 μl of AAV1-hrGFP was used). (**E**) H&E staining of a brain section from a monkey transduced with a high dose of AAV1-hrGFP. Staining shows massive infiltration of macrophages and lymphocytes within the transduced area. Scale bar: 200 μm. (**F**) Higher magnification of the inset from (**E**). Scale bar: 50 μm. (**G**) Perivascular cuffing, an indication of inflammation and an immune response caused by the accumulation of lymphocytes and macrophages in a dense mass around the vessel; representative monkey transduced with low dose of vector. Scale bar: 100 μm. (**H**) H&E staining of the left, control hemisphere, showing no pathology within the infused (PBS) region. Scale bar: 200 μm.

sera still gave a visible signal, whereas group B showed signal only at lower dilutions ($\sim$1:2000). To assess whether AAV1-hrGFP infusion also triggered a cell-mediated immune response, we first stained brain sections for two inflammatory markers: CD68 (macrophages) and Iba-1 (microglia). We detected robust staining against both of these markers only in the right, vector-infused hemisphere of monkeys from group A (Fig. 5A and B). The left, control hemisphere, infused with PBS, showed only localized glial scarring along the needle track. Brain sections from animals that were infused with only 20 μl of the vector into basal forebrain (group B) stained strongly for both CD68 and Iba-1, but this staining was confined to the site of injection (Fig. 5C and D). The difference in the extent of neuroinflammation between these two groups probably results from the different volumes of vector infused (150 vs. 20 μl for groups A and B, respectively). H&E staining confirmed the histopathological changes caused by neuroinflammation that were also proportionate to the dose of vector infused (Fig. 5E–H). Sections from monkeys from group B (low dose) were characterized mainly by the presence of perivascular cuffing—the accumulation of lymphocytes or plasma cells in a dense mass around blood vessels (Fig. 5G). This response was even more evident in animals from group A (high dose). Control hemispheres (infused with PBS) did not show any pathological changes (Fig 5H). A cell-mediated response mounted against the AAV1-hrGFP vector should be evidenced by upregulation of MHC-II in the area of infusion, along with the presence of armed $CD4^+$ lymphocytes. We observed a substantial infiltration of $CD4^+$ cells within the transduced areas as opposed to the contralateral, control hemisphere (Fig. 6A and B). Similarly, a robust signal from the MHC-II marker was detected only within the transduced regions of the brain (Fig. 6C and D). Interestingly, in the brain regions where only neurons were

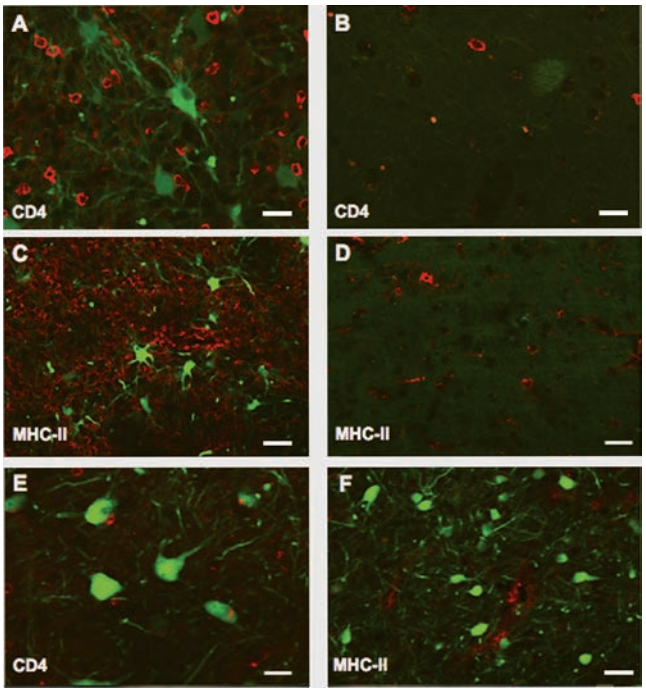

FIG. 6. Neuroinflammation within monkey brain after transduction with AAV1-hrGFP. (**A**) The transduced region of the striatum was massively infiltrated with $CD4^+$ lymphocytes. (**B**) Contralateral, control hemisphere did not show this infiltration. (**C**) Similarly, the transduced region of the striatum showed elevated expression of MHC-II, which was largely absent on the contralateral side (**D**). The transduced subthalamic nucleus did not show massive infiltration of $CD4^+$ lymphocytes (**E**) relative to striatal regions enriched with APCs. MHC-II expression within the subthalamic nucleus (**F**) was not highly elevated in comparison with the striatum or corona radiata. Scale bars: (**A, B**, and **E**) 25 μm; (**C, D**, and **F**) 50 μm.

transduced (e.g., the subthalamic nucleus), only marginal $CD4^+$ infiltration and slightly elevated MHC-II expression could be detected (Fig. 6E and F). Our results indicate that both components (e.g., humoral and cellular) of the adaptive immune system were engaged. The presence of neutralizing and anti-hrGFP antibodies confirms that the immune response is directed against both viral capsid and the foreign transgene. However, it is not clear whether the transgene or the viral capsid plays the major role in the cell-mediated response. We suspect, however, that the transgene is more likely to be driving this response because of the persistent expression of hrGFP, opposed to AAV1 capsids, which do not replicate after cellular transduction and are likely cleared from tissues relatively quickly.

Discussion

In the development of gene therapy approaches for the treatment of various disorders, consideration must be given to various requirements in terms of the specific cell type to be transduced, and the level and range of therapeutic protein necessary to alleviate disease symptoms. Various AAV serotypes have been proposed in different animal models to treat diseases by gene therapy (Halbert *et al.*, 2001; Dodge *et al.*, 2005; Bankiewicz *et al.*, 2006; Inagaki *et al.*, 2006; Tas *et al.*, 2006). The most frequently used serotype in neurological clinical studies has been AAV2 (Fiandaca *et al.*, 2008). Clinical data that has been accrued in more than 100 human subjects indicate the substantial safety of this serotype and mark its emergence as the preferred vector for neurological applications. Much of this apparent safety may be attributed to the remarkable specificity of AAV2 for neurons. This specificity can also be viewed as a limitation. Because only about 20% of brain cells are neurons, the overall level of expression of, say, a secreted factor would necessarily be reduced. In addition, AAV2 would not be able to target oligodendrocytes, for example, of likely relevance in demyelinating diseases such as multiple sclerosis. Such considerations suggest that other serotypes should be explored more extensively, particularly in the primate brain.

A number of reports have shown that the AAV1 serotype transduces the brain more efficiently than does AAV2 (Vite *et al.*, 2003; Wang *et al.*, 2003; Dodge *et al.*, 2005). We have explored in nonhuman primates the utility of this serotype with a vector that encodes a humanized *Renilla* green fluorescent protein (hrGFP) for which the codon usage has been optimized for use in mammals (see patent WO/2004/005322). Our goal was to use this GFP as a marker of cellular transduction to elucidate the types of cells transduced in different parts of the brain, to understand more about how AAV1 is trafficked within and beyond infused brain regions, and to assess the potential safety issues of a vector exhibiting broader tropism than AAV2.

Cellular specificity and vector trafficking

The brain is an extremely heterogeneous composite of distinct structures that are connected by numerous afferent and efferent neurons and interneurons. In addition, the division of the brain into white and gray matter tracts marks distinct physical barriers that impose unique constraints upon the movement of macromolecules and nanoparticles throughout these regions (Krauze *et al.*, 2008). Furthermore, blood vessels clearly play a significant role in the distribution of AAV and other particles over significant distances in the brain (Hadaczek *et al.*, 2006b). We have shown previously that pulse pressure seems to be an important driver of convective distribution, and have termed this the *perivascular pump*. Finally, differential distribution of cellular AAV receptors, such as heparan sulfate proteoglycan (HSPG) for AAV2 (Summerford and Samulski, 1998) and α-2,3 and α-2,6 N-linked sialic acids for AAV1 (Wu *et al.*, 2006b), can both affect vector trafficking and cellular specificity. Various coinfusates, such as heparin and basic fibroblast growth factor (bFGF), can be used to block the binding temporarily, thereby allowing AAV2 particles to spread further into the brain parenchyma (Nguyen *et al.*, 2001; Mastakov *et al.*, 2002; Hadaczek *et al.*, 2004), although similar techniques have not been reported for AAV1.

To understand the distribution of AAV1 in various regions of the primate brain, we targeted three regions: the striatum, corona radiata, and basal forebrain. The gray matter of the putamen has been the anatomical target of two AAV2-based clinical trials for Parkinson's disease (Fiandaca *et al.*, 2008), and transduces well because of the abundant presence of

neuronal cell bodies. AAV1-hrGFP also transduced the putamen well. However, in striking contrast to our experience with AAV2, AAV1-hrGFP evinced a remarkable preference for striatal astrocytes. This preference for astrocytes over neurons was not seen in the basal forebrain, where neurons were favored strongly over astrocytes. The reason for this phenomenon is unclear. However, it may be related to differences in neuronal phenotype from one region to another. In fact, this idea finds further support in the fact that trafficking of vector from the striatum to the subthalamic nucleus and globus pallidus results in preferential neuronal transduction rather than the virtually exclusive astrocytic transduction seen in the putamen and caudate (Fig. 3D–I). Interestingly, when the same vector was infused into mouse brain (McBride *et al.*, 2008), robust expression of GFP was also observed in cells throughout the whole striatum and globus pallidus. However, the positive cells were clearly neurons ($NeuN^+$), a strikingly different outcome from our results. As mentioned previously, it may be due to differences in neuronal phenotypes between two species (e.g., monkey vs. mouse).

The constituent structures of the basal ganglia are interconnected by both afferent and efferent neurons. When monkey striatum (caudate and putamen) was infused, strong hrGFP fluorescence was detected also in the external and internal parts of the globus pallidus, the subthalamic nucleus, the medial forebrain bundle, and both the internal capsule and anterior commissure. Retrograde neuronal transport of AAV2 along motor neurons has been reported by others (Kaspar *et al.*, 2002) and this may also take place also in the case of AAV1. However, this cannot be the mechanism at work in the striatum because we detected no neuronal transduction in the striatum. We have previously described a perivascular pump powered by pulsing blood vessels to move vector along vascular tracts (Hadaczek *et al.*, 2006b). This underappreciated mechanism for convective distribution of AAV and other substances is, in our view, the most likely explanation for trafficking of vector throughout the basal ganglia.

When the corona radiata (CR) was infused, vector was distributed widely and remained mostly within the infused structure. On the basis of DAPI staining, almost half of the cells within the CR were transduced. Double staining with Olig2 and hrGFP antibodies confirmed that the great majority (88%) of transduced cells were oligodendrocytes, further confirming AAV1 tropism for glial cells (astrocytes and oligodendrocytes). It has been reported that AAV can efficiently drive expression in oligodendrocytes only when the myelin basic protein (MBP) promoter is used in the expression cassette (Chen *et al.*, 1999). However, in our hands, the CMV promoter worked well in driving hrGFP expression in oligodendrocytes.

One of the most striking phenomena observed in this study was the spread of hrGFP from the corona radiata to the deep layers of cortical neurons neighboring the infused structure. Almost 40% of the neurons located at the border with CR were transduced with AAV1. This transition from primarily oligodendrocytic transduction in the CR to primarily neuronal transduction in adjacent cortical layers mirrors the switch in cellular specificity from astrocytes to neurons in the striatal infusions. Infusions of therapeutic vectors into the corona radiata could potentially serve as a conduit to spread vectors efficiently, and thereby transduce neurons across large areas of the cortex. This might be especially important for diseases for which global delivery would be required (Huntington's, Alzheimer's, Niemann–Pick disease, etc.).

Immune response

A major challenge in optimizing viral vectors for gene therapy relates to the immune/inflammatory response of the host. The robust transduction of glia in our initial staining experiments alerted us to the possible transduction of antigen-presenting cells within the CNS. Immunogenicity of both GFP (Stripecke *et al.*, 1999; Gambotto *et al.*, 2000; Re *et al.*, 2004) and AAV1 capsid (Zaiss and Muruve, 2008) has previously been reported. All monkeys in the present study acquired circulating antibodies against both AAV1 capsid and hrGFP transgene by 1 month after vector infusion, irrespective of the brain region infused. Animals that received only 20 μl of AAV1-hrGFP in the basal forebrain, rather than the 150 μl delivered to the CR or striatum, had lower titers of antibodies against capsid and transgene, indicating that immune response was dependent on vector dose and not on site of infusion or other factors.

As we suspected, monkeys from group A exhibited a strong inflammatory reaction in the brain. Staining of brain sections with anti-CD68 (macrophages) and anti-Iba-1 (microglia) indicated substantial neuroinflammation proportional to the amount of vector infused. Histopathological changes with characteristic perivascular cuffing were also confirmed by H&E staining. If AAV1-hrGFP transduction of APCs in the brain were triggering a cell-mediated immune response, we would expect to see infiltration of $CD4^+$ T lymphocytes. Such infiltration was seen strongly in regions of the brain in which nonneuronal cells were transduced, but to a much lesser extent in areas in which only neurons were transduced. For example, the striatum contained $CD4^+$ cells but the subthalamic nucleus, containing only transduced neurons, did not. This result illustrates the fact that neurons are not professional APCs, and that they are not targeted by armed T cells. We also saw upregulation of MHC-II in endothelial cells, suggesting function for these cells as APCs (Cornet *et al.*, 2000; Constantinescu *et al.*, 2005). This creates an apparent paradox because we saw no cells that were positive for both hrGFP and MHC-II. One possible explanation for this is that APCs actively presenting hrGFP peptides may have been eliminated by the invading T cells in the month following vector infusion.

We showed in this study that, like AAV2-based vectors, AAV1 transduces neurons. Also like AAV2, it can be trafficked efficiently to distal functionally linked sites. The dramatic change in cellular specificity that accompanied this trafficking is a new finding that may be visible only within the context of a large primate brain. But it suggests that phenotypic differences in neurons, dependent on anatomic location and functional specialization, may play a more significant role in transduction specificity than previously thought. Finally, the ability of AAV1 to transduce nonneuronal cells may trigger a much stronger immune response mediated by APCs in the brain, although this phenomenon doubtless depends on the immunogenicity of the transgene. Therefore, when using AAV1 as a platform in gene therapy, caution must be exercised in the design and interpretation of experiments and

investigators must be careful about choosing the right reporter gene, as it may trigger a robust immune/inflammatory response not seen with AAV2 vector.

Acknowledgments

Funding from Hereditary Disease Foundation and Targeted Genetics Corporation supported this study.

Author Disclosure Statement

No competing financial interests exist.

References

Bankiewicz, K.S., Eberling, J.L., Kohutnicka, M., Jagust, W., Pivirotto, P., Bringas, J., Cunningham, J., Budinger, T.F., and Harvey-White, J. (2000). Convection-enhanced delivery of AAV vector in parkinsonian monkeys: *In vivo* detection of gene expression and restoration of dopaminergic function using pro-drug approach. Exp. Neurol. 164, 2–14.

Bankiewicz, K.S., Daadi, M.M., Pivirotto, P., Bringas, J., Sanchez-Pernaute, R., Herscovitch, P., Carson, R., Eckelman, W., Cunningham, J., Reutter, B., Vanbrocklin, H.F., and Eberling, J.L. (2003). Long term evaluation of AAV/AADC gene transfer in parkinsonian monkeys. Presented at the 33rd Annual Meeting of the Society for Neuroscience (Neuroscience, Washington, DC). Program no. 299.214.

Bankiewicz, K.S., Forsayeth, J., Eberling, J.L., Sanchez-Pernaute, R., Pivirotto, P., Bringas, J., Herscovitch, P., Carson, R.E., Eckelman, W., Reutter, B., and Cunningham, J. (2006). Long-term clinical improvement in MPTP-lesioned primates after gene therapy with AAV-hAADC. Mol. Ther. 14, 564–570.

Bobo, R.H., Laske, D.W., Akbasak, A., Morrison, P.F., Dedrick, R.L., and Oldfield, E.H. (1994). Convection-enhanced delivery of macromolecules in the brain. Proc. Natl. Acad. Sci. U.S.A. 91, 2076–2080.

Burger, C., Gorbatyuk, O.S., Velardo, M.J., Peden, C.S., Williams, P., Zolotukhin, S., Reier, P.J., Mandel, R.J., and Muzyczka, N. (2004). Recombinant AAV viral vectors pseudotyped with viral capsids from serotypes 1, 2, and 5 display differential efficiency and cell tropism after delivery to different regions of the central nervous system. Mol. Ther. 10, 302–317.

Cavalieri, B. (1996). *Geometria Degli Indivisible* (Unione Tipografica Editrice, Turin, Italy).

Chen, H., McCarty, D.M., Bruce, A.T., and Suzuki, K. (1999). Oligodendrocyte-specific gene expression in mouse brain: Use of a myelin-forming cell type-specific promoter in an adeno-associated virus. J. Neurosci. Res. 55, 504–513.

Constantinescu, C.S., Tani, M., Ransohoff, R.M., Wysocka, M., Hilliard, B., Fujioka, T., Murphy, S., Tighe, P.J., Sarma, J.D., Trinchieri, G., and Rostami, A. (2005). Astrocytes as antigen-presenting cells: Expression of IL-12/IL-23. J. Neurochem. 95, 331–340.

Cornet, A., Bettelli, E., Oukka, M., Cambouris, C., Avellana-Adalid, V., Kosmatopoulos, K., and Liblau, R.S. (2000). Role of astrocytes in antigen presentation and naive T-cell activation. J. Neuroimmunol. 106, 69–77.

Cunningham, J., Oiwa, Y., Nagy, D., Podsakoff, G., Colosi, P., and Bankiewicz, K.S. (2000). Distribution of AAV-TK following intracranial convection-enhanced delivery into rats. Cell Transplant. 9, 585–594.

Cunningham, J., Pivirotto, P., Bringas, J., Suzuki, B., Vijay, S., Sanftner, L., Kitamura, M., Chan, C., and Bankiewicz, K.S. (2008). Biodistribution of adeno-associated virus type-2 in nonhuman primates after convection-enhanced delivery to brain. Mol. Ther. 16, 1267–1275.

Davidson, B.L., and Breakefield, X.O. (2003). Viral vectors for gene delivery to the nervous system. Nat. Rev. Neurosci. 4, 353–364.

Davidson, B.L., Stein, C.S., Heth, J.A., Martins, I., Kotin, R.M., Derksen, T.A., Zabner, J., Ghodsi, A., and Chiorini, J.A. (2000). Recombinant adeno-associated virus type 2, 4, and 5 vectors: Transduction of variant cell types and regions in the mammalian central nervous system. Proc. Natl. Acad. Sci. U.S.A. 97, 3428–3432.

Dodge, J.C., Clarke, J., Song, A., Bu, J., Yang, W., Taksir, T.V., Griffiths, D., Zhao, M.A., Schuchman, E.H., Cheng, S.H., O'Riordan, C.R., Shihabuddin, L.S., Passini, M.A., and Stewart, G.R. (2005). Gene transfer of human acid sphingomyelinase corrects neuropathology and motor deficits in a mouse model of Niemann–Pick type A disease. Proc. Natl. Acad. Sci. U.S.A. 102, 17822–17827.

Fiandaca, M., Forsayeth, J., and Bankiewicz, K. (2008). Current status of gene therapy trials for Parkinson's disease. Exp. Neurol. 209, 51–57.

Gambotto, A., Dworacki, G., Cicinnati, V., Kenniston, T., Steitz, J., Tuting, T., Robbins, P.D., and Deleo, A.B. (2000). Immunogenicity of enhanced green fluorescent protein (EGFP) in BALB/c mice: Identification of an H2-K^d-restricted CTL epitope. Gene Ther. 7, 2036–2040.

Gao, G., Vandenberghe, L.H., and Wilson, J.M. (2005). New recombinant serotypes of AAV vectors. Curr. Gene Ther. 5, 285–297.

Grimm, D., and Kay, M.A. (2003). From virus evolution to vector revolution: Use of naturally occurring serotypes of adeno-associated virus (AAV) as novel vectors for human gene therapy. Curr. Gene Ther. 3, 281–304.

Hadaczek, P., Mirek, H., Bringas, J., Cunningham, J., and Bankiewicz, K. (2004). Basic fibroblast growth factor enhances transduction, distribution, and axonal transport of adeno-associated virus type 2 vector in rat brain. Hum. Gene Ther. 15, 469–479.

Hadaczek, P., Kohutnicka, M., Krauze, M.T., Bringas, J., Pivirotto, P., Cunningham, J., and Bankiewicz, K. (2006a). Convection-enhanced delivery of adeno-associated virus type 2 (AAV2) into the striatum and transport of AAV2 within monkey brain. Hum. Gene Ther. 17, 291–302.

Hadaczek, P., Yamashita, Y., Mirek, H., Tamas, L., Bohn, M.C., Noble, C., Park, J.W., and Bankiewicz, K. (2006b). The "perivascular pump" driven by arterial pulsation is a powerful mechanism for the distribution of therapeutic molecules within the brain. Mol. Ther. 14, 69–78.

Halbert, C.L., Allen, J.M., and Miller, A.D. (2001). Adeno-associated virus type 6 (AAV6) vectors mediate efficient transduction of airway epithelial cells in mouse lungs compared to that of AAV2 vectors. J. Virol. 75, 6615–6624.

Inagaki, K., Fuess, S., Storm, T.A., Gibson, G.A., McTiernan, C.F., Kay, M.A., and Nakai, H. (2006). Robust systemic transduction with AAV9 vectors in mice: Efficient global cardiac gene transfer superior to that of AAV8. Mol. Ther. 14, 45–53.

Kaludov, N., Handelman, B., and Chiorini, J.A. (2002). Scalable purification of adeno-associated virus type 2, 4, or 5 using ion-exchange chromatography. Hum. Gene Ther. 13, 1235–1243.

Kaplitt, M.G., Leone, P., Samulski, R.J., Xiao, X., Pfaff, D.W., O'Malley, K.L., and During, M.J. (1994). Long-term gene expression and phenotypic correction using adeno-associated virus vectors in the mammalian brain. Nat. Genet. 8, 148–154.

Kaspar, B.K., Erickson, D., Schaffer, D., Hinh, L., Gage, F.H., and Peterson, D.A. (2002). Targeted retrograde gene delivery for neuronal protection. Mol. Ther. 5, 50–56.

Krauze, M.T., McKnight, T.R., Yamashita, Y., Bringas, J., Noble, C.O., Saito, R., Geletneky, K., Forsayeth, J., Berger, M.S., Jackson, P., Park, J.W., and Bankiewicz, K.S. (2005). Real-time visualization and characterization of liposomal delivery into the monkey brain by magnetic resonance imaging. Brain Res. Brain Res. Protoc. 16, 20–26.

Krauze, M.T., Vandenberg, S.R., Yamashita, Y., Saito, R., Forsayeth, J., Noble, C., Park, J., and Bankiewicz, K.S. (2008). Safety of real-time convection-enhanced delivery of liposomes to primate brain: A long-term retrospective. Exp. Neurol. 210, 638–644.

Lieberman, D.M., Laske, D.W., Morrison, P.F., Bankiewicz, K.S., and Oldfield, E.H. (1995). Convection-enhanced distribution of large molecules in gray matter during interstitial drug infusion. J. Neurosurg. 82, 1021–1029.

Mastakov, M.Y., Baer, K., Kotin, R.M., and During, M.J. (2002). Recombinant adeno-associated virus serotypes 2- and 5-mediated gene transfer in the mammalian brain: Quantitative analysis of heparin co-infusion. Mol. Ther. 5, 371–380.

McBride, J.L., Boudreau, R.L., Harper, S.Q., Staber, P.D., Monteys, A.M., Martins, I., Gilmore, B.L., Burstein, H., Peluso, R.W., Polisky, B., Carter, B.J., and Davidson, B.L. (2008). Artificial miRNAs mitigate shRNA-mediated toxicity in the brain: Implications for the therapeutic development of RNAi. Proc. Natl. Acad. Sci. U.S.A. 105, 5868–5873.

Mori, S., Wang, L., Takeuchi, T., and Kanda, T. (2004). Two novel adeno-associated viruses from cynomolgus monkey: Pseudotyping characterization of capsid protein. Virology 330, 375–383.

Nguyen, J.B., Sanchez-Pernaute, R., Cunningham, J., and Bankiewicz, K.S. (2001). Convection-enhanced delivery of AAV-2 combined with heparin increases TK gene transfer in the rat brain. Neuroreport 12, 1961–1964.

Passini, M.A., MaCauley, S.L., Huff, M.R., Taksir, T.V., Bu, J., Wu, I.H., Piepenhagen, P.A., Dodge, J.C., Shihabuddin, L.S., O'Riordan, C.R., Schuchman, E.H., and Stewart, G.R. (2005). AAV vector-mediated correction of brain pathology in a mouse model of Niemann–Pick A disease. Mol. Ther. 11, 754–762.

Re, F., Srinivasan, R., Igarashi, T., Marincola, F., and Childs, R. (2004). Green fluorescent protein expression in dendritic cells enhances their immunogenicity and elicits specific cytotoxic T-cell responses in humans. Exp. Hematol. 32, 210–217.

Saito, R., Krauze, M.T., Bringas, J.R., Noble, C., McKnight, T.R., Jackson, P., Wendland, M.F., Mamot, C., Drummond, D.C., Kirpotin, D.B., Hong, K., Berger, M.S., Park, J.W., and Bankiewicz, K.S. (2005). Gadolinium-loaded liposomes allow for real-time magnetic resonance imaging of convection-enhanced delivery in the primate brain. Exp. Neurol. 196, 381–389.

Samulski, R.J., Berns, K.I., Tan, M., and Muzyczka, N. (1982). Cloning of adeno-associated virus into pBR322: Rescue of intact virus from the recombinant plasmid in human cells. Proc. Natl. Acad. Sci. U.S.A. 79, 2077–2081.

Samulski, R.J., Srivastava, A., Berns, K.I., and Muzyczka, N. (1983). Rescue of adeno-associated virus from recombinant plasmids: Gene correction within the terminal repeats of AAV. Cell 33, 135–143.

Sanftner, L.M., Suzuki, B.M., Doroudchi, M.M., Feng, L., McClelland, A., Forsayeth, J.R., and Cunningham, J. (2004). Striatal delivery of rAAV-hAADC to rats with preexisting immunity to AAV. Mol. Ther. 9, 403–409.

Stripecke, R., Carmen Villacres, M., Skelton, D., Satake, N., Halene, S., and Kohn, D. (1999). Immune response to green fluorescent protein: Implications for gene therapy. Gene Ther. 6, 1305–1312.

Summerford, C., and Samulski, R.J. (1998). Membrane-associated heparan sulfate proteoglycan is a receptor for adeno-associated virus type 2 virions. J. Virol. 72, 1438–1445.

Tas, S.W., Adriaansen, J., Hajji, N., Bakker, A.C., Firestein, G.S., Vervoordeldonk, M.J., and Tak, P.P. (2006). Amelioration of arthritis by intraarticular dominant negative IKKβ gene therapy using adeno-associated virus type 5. Hum. Gene Ther. 17, 821–832.

Vite, C.H., Passini, M.A., Haskins, M.E., and Wolfe, J.H. (2003). Adeno-associated virus vector-mediated transduction in the cat brain. Gene Ther. 10, 1874–1881.

Wang, C., Wang, C.M., Clark, K.R., and Sferra, T.J. (2003). Recombinant AAV serotype 1 transduction efficiency and tropism in the murine brain. Gene Ther. 10, 1528–1534.

Wu, Z., Asokan, A., and Samulski, R.J. (2006a). Adeno-associated virus serotypes: Vector toolkit for human gene therapy. Mol. Ther. 14, 316–327.

Wu, Z., Miller, E., Agbandje-McKenna, M., and Samulski, R.J. (2006b). α2,3 and α2,6 N-linked sialic acids facilitate efficient binding and transduction by adeno-associated virus types 1 and 6. J. Virol. 80, 9093–9103.

Zaiss, A.K., and Muruve, D.A. (2008). Immunity to adeno-associated virus vectors in animals and humans: A continued challenge. Gene Ther. 15, 808–816.

Zolotukhin, S., Potter, M., Zolotukhin, I., Sakai, Y., Loiler, S., Fraites, T.J., Jr., Chiodo, V.A., Phillipsberg, T., Muzyczka, N., Hauswirth, W.W., Flotte, T.R., Byrne, B.J., and Snyder, R.O. (2002). Production and purification of serotype 1, 2, and 5 recombinant adeno-associated viral vectors. Methods 28, 158–167.

Address reprint requests to:
Dr. Piotr Hadaczek
Laboratory of Molecular Therapeutics
Department of Neurological Surgery
University of California, San Francisco
MCB, 1855 Folsom Street, Room 226
San Francisco, CA 94103

E-mail: piotr.hadaczek@ucsf.edu

Received for publication September 16, 2008;
accepted after revision December 12, 2008.

Published online: January 30, 2009.